

Nanolithographic Top-Down Patterning of Polyoxovanadate-Based Nanostructures with Switchable Electrical Resistivity

Benedikt Rösner,^{*[a]} Roberto Fallica,^[a] Manuel Johnson,^[b] Andreas Späth,^[b] Rainer Fink,^[b] Yasin Ekinci,^[a] Christian David,^[a] Montaha H. Anjass,^[c, d] and Carsten Streb^[c, d]

Abstract: The top-down lithographic fabrication of functional metal oxide nanostructures enables technologically important applications such as catalysis and electronics. Here, we report the use of molecular vanadium oxides, polyoxovanadates, as molecular precursors for electron beam lithography to obtain functional vanadium oxide nanostructures. The new resist class described gives access to nanostructures with minimum dimensions close to 10 nm. The lithographically prepared structures exhibit temperature-dependent switching behaviour of their electrical resistivity. The work could lay the foundation for accessing functional vanadium oxide nanostructures in the sub-10-nm domain using industrially established nanolithographic methods.

The ability to design metal oxide nanostructures is a key technology for applications ranging from catalysis and sensing through to molecular electronics and data storage. Molecular metal oxides, so-called polyoxometalates (POMs),^[1] are frequently used as molecular precursors for the preparation of metal oxide nanostructures.^[2] POMs are anionic metal oxide clusters based on early transition metals (mainly Mo, W, V) which can be functionalized with most metals from the periodic table, thus giving access to a wide range of molecular metal oxide precursors. In addition, POM-solubility in a wide range of solvents can be tuned by cation modification.^[3] Based on their

molecular nature, POMs are an ideal class of molecular precursors as negative-tone materials for methods based on direct patterning, as they can be dissolved in a wide range of industrial solvents including water, and their structure, chemical composition, and photochemical reactivity can be tuned by chemical modification. To date, POMs are typically used in bottom-up self-assembly to access nanostructures ranging from 1D chains through to 2D films and 3D frameworks.^[2,4] These systems often link structure and function, so that applications in energy conversion/storage,^[5] molecular electronics,^[6] bio-medicine^[7] and nanostructuring^[8] have recently been established. In contrast, targeted top-down nanofabrication approaches based on functional POMs are virtually unknown.^[9] Making POMs amenable to these nanostructuring methods is, however, highly attractive for technologic applications, as it will combine the exceptionally high spatial resolution of lithography processes with the ability to design functional nanoscale devices in virtually any geometry. To this end, the integration of POMs into extreme ultraviolet (EUV) lithography or electron beam lithography (EBL) is a key challenge for top-down nanofabrication with use in semiconductor technology,^[10] or the design of functional nano-architectures.^[11] To date, academia and industry invest tremendous efforts to push the frontiers of lithography to ever smaller structures by developing cutting-edge exposure tools, optics, masks, and resist materials.^[12] The use of novel classes of POMs as resist materials for lithographic techniques could therefore open new pathways to metal oxide nanostructures with high functionality, defined geometries and patterning resolution down to the sub-10 nm regime with applications ranging from electronics and semiconductors to catalysis and energy storage.^[13]


This concept is based on recent studies which have used hybrid resists consisting of inorganic and organic components, which serve as hard masks for subsequent surface patterning processes.^[14] In this approach, the organic component is decomposed by exposure to photon radiation, an electron or ion beam, while the inorganic counterpart undergoes condensation reactions leading to the formation of a solid-state network (Figure 1). Once the exposed material is treated with a suitable developer (typically mineral acids or bases), the non-exposed molecular components are dissolved and removed from the sample, while the exposed, solid-state components are retained. This scheme enables direct patterning, referred to as negative-tone patterning in lithography. The combination of high resolution, high etch resistance, scalability, and compatibility with existing processes makes the new hybrid resist materials technologically attractive for large-scale manufacturing by EUV lithography.^[15] These broad requirements have led


[a] Dr. B. Rösner, Dr. R. Fallica, Dr. Y. Ekinci, Dr. C. David
Paul Scherrer Institut
5232 Villigen PSI (Switzerland)
E-mail: benedikt.rosner@psi.ch

[b] M. Johnson, Dr. A. Späth, Prof. Dr. R. Fink
Department Chemie und Pharmazie
Friedrich-Alexander-Universität (FAU) Erlangen-Nürnberg
Egerlandstraße 3, 91058 Erlangen (Germany)

[c] Dr. M. H. Anjass, Prof. Dr. C. Streb
Institute of Inorganic Chemistry I
Ulm University
Albert-Einstein-Allee 47, 89081 Ulm (Germany)
E-mail: carsten.streb@uni-ulm.de

[d] Dr. M. H. Anjass, Prof. Dr. C. Streb
Helmholtz Institute Ulm
Electrochemical Energy Storage
Helmholtzstr. 11, 89081 Ulm (Germany)

 Supporting information for this article is available on the WWW under <https://doi.org/10.1002/cnma.202000425>

 © 2020 The Authors. Published by Wiley-VCH GmbH. This is an open access article under the terms of the Creative Commons Attribution License, which permits use, distribution and reproduction in any medium, provided the original work is properly cited.

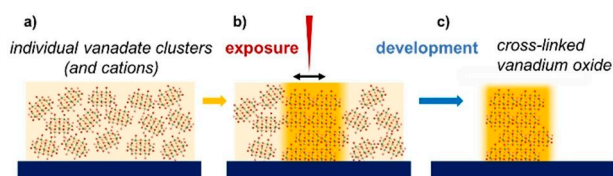


Figure 1. Schematic illustration of electron beam lithography with a negative-tone resist based on vanadate building blocks. a) A solution of vanadate clusters with their counter ions and surfactants is deposited on a clean surface. b) The material is exposed with a focused electron beam and subsequently developed. c) The unexposed material is dissolved and removed, leaving a patterned structure of the unsolvable material that has been cross-linked in the lithographic process behind.

to the development of hydrogen silsesquioxane (HSQ) as prototype negative-tone resist in nanolithography which combines well-established chemical properties with facile processing, good etch resistivity and high lithographic resolution.^[16] However, the resulting silicon oxide nanostructures offer limited chemical reactivity, so that next-generation resists with added functionalities (e.g. redox- or acid/base-reactivity) are required to open new application scenarios, such as catalysis, or integration in electrical circuits. Pioneering studies in this direction have developed alternative resists with (photo)catalytic or redox-properties based on metal-oxide organic clusters,^[17] metal-oxide cores,^[18] as well as molecular metal oxides (polyoxometalates, POMs).^[15a,19]

In particular, molecular vanadium oxides (polyoxovanadates) are ideal prototype molecules for the requirements described above, as their deposition on flat surfaces as well as their conversion into solid-state vanadium oxide nanostructures by heat,^[20] irradiation^[8a] or even sonication^[21] is well documented in the literature. In addition, polyoxovanadates offer very high absorbance in the UV region due to O→M ligand-to-metal charge-transfer (LMCT) transitions, an effect that is exploited in a range of highly sensitive EUV resists.^[22] The resulting vanadium oxides are one of the technologically most important metal oxide classes, with applications ranging from oxidation catalysis and photocatalysis to electronics, semiconductors, and batteries.^[23]

The ability to deposit these functional metal oxide nanostructures with (photo)catalytic activity or redox-properties by lithography has led to pioneering studies into alternative resists based on metal-oxide organic clusters,^[17] metal-oxide cores,^[18] as well as molecular metal oxides (polyoxometalates, POMs).^[15a,19] Inspired by the early studies of POM-resists, we report the first example of polyoxovanadate-based negative-tone resists. Here, we used the polyoxovanadate prototype cluster^[24] $[V_4O_{12}]^{4-}$ as a vanadium oxide precursor and demonstrate its incorporation in a new resist suitable for EBL. We emphasize that the focus of this study lies on the direct patterning of functional structures rather than the use of such structures for pattern transfer. Achieving structure sizes down to 10 nm is possible without optimization of the resist composition, paving the way for a new class of functional metal oxide materials that can directly form nanostructures. An

example of such structures is the direct use of nanostructures that are fabricated from the negative-tone electron lithography resist HSQ as diffractive optical element.^[25]

In our study, we use a resist preparation based on earlier works on alumina-based resists.^[26] In short, $(nBu_4N)_4[V_4O_{12}]^{24}$ was dissolved in 2-methoxyethanol containing acetic acid and triethoxyphenyl silane (detailed description in Experimental Section). Since no prior information on polyoxovanadate-based resists is available, we systematically optimized the processing parameters including pre- and post-bake temperatures, type of developer and development time.

To characterize the behaviour of the non-optimized prototype material upon electron exposure and development, we investigated its sensitivity to electron dose and critical dimensions, *i.e.*, the minimum of achievable structure sizes. A contrast curve was obtained by examination of a dose series that was exposed as squares of 25 μm edge length, using electrons accelerated with 100 kV. The series covered a dose range from 1–64 mC/cm^2 . Figure 2 shows the average height of each square as determined using a profilometer. Atomic force microscopy (AFM) was used to confirm the height of the selected squares (Figure 2, inset). We observe the formation of a uniform, non-cracked film with an average thickness of 19.8 ± 0.6 nm. This height is reached at an exposure dose of 42 mC/cm^2 , which is a factor two to four higher compared to established resist materials based on oxidic clusters such as HSQ. These values show indeed comparably poor contrast and sensitivity to electrons of our prototype material as in many other cases of inorganic resist materials, but still offer optimization potential of the present system in terms of sensitivity.

Besides contrast and sensitivity, we evaluated the maximum resolution accessible with the vanadate resist. To this end, we exposed so-called Siemens stars as test patterns with a programmed minimum line width of five nanometres (Figure 3). The low-magnification SEM images of the Siemens star (Figure 3a, b) show that the resist forms vanadium oxide structures on a micro- and nanoscale that are stably attached to the Si substrate. The zoomed-in views (Figure 3c, d) disclose that the resist is capable of forming fine structures approaching the ten-

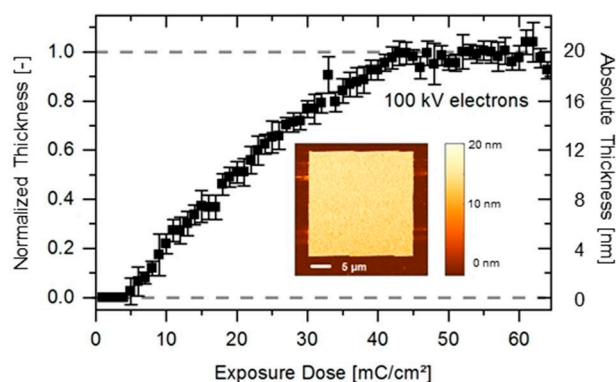


Figure 2. Contrast curve for electron beam lithography of the resist using exposure doses of 1–64 mC/cm^2 (acceleration voltage: 100 keV) on squares of $25 \times 25 \mu\text{m}$ (inset shows an AFM height map).

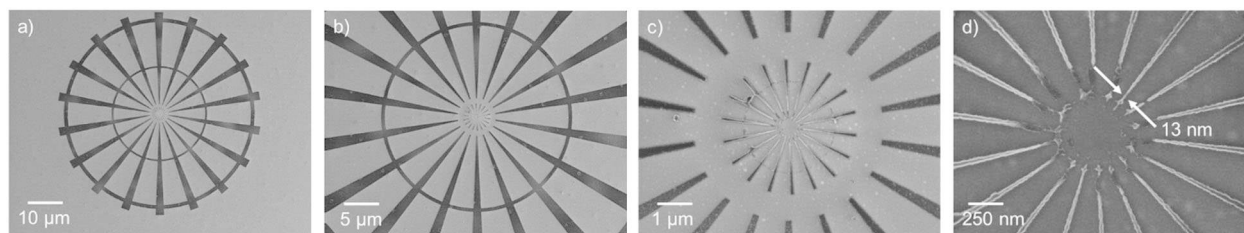


Figure 3. SEM images of a Siemens star resolution test pattern. a) Overview micrograph; b) zoom into the inner region; c) detailed image of the innermost ring; d) close-up view of the innermost spokes of the Siemens star. The smallest stable structures have a line width of 13 nm. Note that the inner ring (which is almost completely removed) represents a line width of 10 nm.

nanometre resolution level. The finest stable structures found in the Siemens star test patterns were 13 nm wide and 50 nm high. The aspect ratios that can be achieved under these conditions are thus between three and four. Structures with lower line widths were either removed by the developer or collapsed.

To gain further insights into the patterning behaviour of our resist, we examined a test pattern that was designed with dense and isolated lines (see Figure 4). For a pitch of 60 nm (i.e. the distance of the repetition of the lines), the resulting line pattern is clean and stable, and shows a line width of 16 nm (corresponding to a fill factor of 27%, Figure 4a). We have to note that the exposure and development conditions are chosen to reach the plateau of the contrast curve. Thus, we do not present structures that show real half-pitch dimensions as usually referred to in dense line patterns. At a pitch of 44 nm, the lines are notably rougher, while the line width remains almost constant (15 nm, fill factor 34%, Figure 4b). Finally, the smallest structures were found at a pitch of 32 nm, with 11.5 nm line width (fill factor 36%, Figure 4c). At these dimensions, we observe significant line roughness and distortions, and a few instances of collapse are observed in the pattern with neighbouring lines. The isolated line, albeit quite rough, is stable and free of defects.

These promising initial results show that, while further optimization in terms of sensitivity and optimum processing parameters is required, the high structural resolution and observed stability promise a direct and powerful method to

pattern functional vanadium oxide nanostructures. This is of particular interest since vanadium oxides of several stoichiometries and oxidation states can undergo a phase transition above room temperature (60–80 °C), turning from an insulator to a semiconductor or even a metallic conductor,^[27] which could be used to access resistive switching devices for future electronics. To characterize the conductivity and resistive behaviour of our nanostructures after the lithography step, we deposited 5 μm wide stripes of vanadium oxide on gold electrodes (channel width 5 μm, in-line arrangement of four electrodes for four-point probe measurements). We hypothesized that a high carbon content is unfavourable for charge transport, and therefore substituted the $(n\text{Bu}_4\text{N})_4[\text{V}_4\text{O}_{12}]$ precursor with the carbon-free species $\text{Li}_6[\text{V}_{10}\text{O}_{28}]\cdot x(\text{H}_2\text{O})_{16}$.^[20b] Figure 5 shows the temperature dependence of the resistivity of nanostructures fabricated from both materials. Control experiments with the unexposed material show a resistivity that is out of measurement range.

We observe indeed that the nanostructures that were deposited from the carbon-rich precursor material show only a poor temperature dependence: the resistivity is slightly reduced at temperatures higher than 60 °C. In contrast, the material with less carbon content shows a more distinct change in resistivity, although the ratio between the two states remains within one order of magnitude. However, a quantification whether this arises from the lower carbon content or a different vanadium oxide composition remains an open question for further study. Nevertheless, the results indicate that the developed nano-

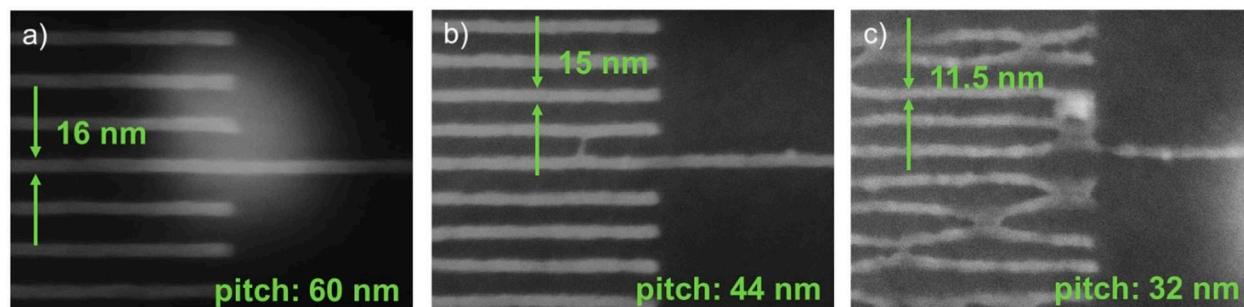


Figure 4. Test pattern that is designed with dense and isolated lines. a) A defect-free structure with 60 nm pitch and 16 nm line width. b) A pitch of 44 nm results in 15 nm lines with decreased structural quality. c) At a pitch of 32 nm, structurally poor lines with a line width of 11.5 nm are observed.

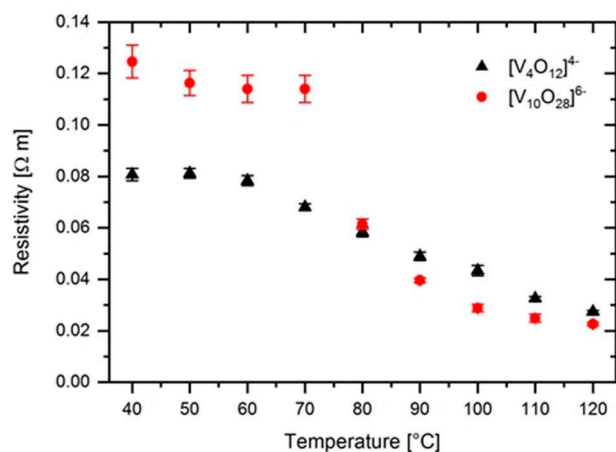


Figure 5. Temperature dependence of the resistivity of exposed and developed structures fabricated from both vanadium precursors. The measurements were conducted by voltage sweeps and linear fits. The precursor with four vanadium centres with the higher carbon content did not show a clear threshold temperature for resistivity switching (black), whereas the processed structures from the carbon-free lithium-based precursor molecule (red) show a distinct resistivity switching temperature between 70° and 80 °C.

structures could exhibit similar resistivity switching mechanism as reported in the literature for bulk and thin film vanadium oxide. Thus, this nanomaterial offers new possibilities for the design of functional electronic devices.

In summary, we present the first example of a polyoxovanadate-based negative-tone resist suitable for preparing nanoscale vanadium oxide structures by electron-beam lithography. The direct and facile incorporation of the resist into the established lithographic techniques was achieved, enabling the fabrication of high-fidelity structures with structure sizes approaching 10 nm. Given the wide range of available polyoxovanadates and heterometallic derivatives, materials optimization seems plausible to give pure vanadium oxide, doped vanadium oxide, or mixed metal oxide nanostructures below the 10 nm resolution. Moreover, we successfully demonstrated that the resistivity of such nanostructures can be manipulated by temperature. This opens a range of possibilities in nanostructured electronic devices, for instance, the incorporation of safety elements that would shortcut a heat-sensitive circuit at a moderate threshold temperature around 70 °C. Future work will involve the optimization of the current system to overcome the current limitations in film homogeneity and aggregate formation, so that access to large-area functional metal oxide nanostructures becomes possible.

Acknowledgements

Atomic force microscopy was performed at the Scanning Probe Microscopy Laboratory of PSI. We acknowledge supporting measurements at the SEM by Dimitris Kazazis. This project has received funding from the EU-H2020 research and innovation programme under grant agreement No654360 NFFA-Europe. CS

gratefully acknowledges financial support by Ulm University, the Helmholtz-Gemeinschaft (HGF) and the Deutsche Forschungsgemeinschaft DFG (STR1164/12).

Conflict of Interest

The authors declare no conflict of interest.

Keywords: Polyoxometalates · Vanadium Oxide · Nanostructure · Self-Assembly · Metal Oxide

- [1] L. Cronin, A. Müller, *Chem. Soc. Rev.* **2012**, *41*, 7325–7326.
- [2] a) P. Kögerler, L. Cronin, *Angew. Chem. Int. Ed.* **2005**, *44*, 844–846; *Angew. Chem.* **2005**, *117*, 866–868; b) D.-L. Long, E. Burkholder, L. Cronin, *Chem. Soc. Rev.* **2007**, *36*, 105–121; c) Y. Ji, L. Huang, J. Hu, C. Streb, Y.-F. Song, *Energy Environ. Sci.* **2015**, *8*, 776–789.
- [3] a) S. Herrmann, M. Kostrzewa, A. Wierschem, C. Streb, *Angew. Chem. Int. Ed.* **2014**, *53*, 13596–13599; *Angew. Chem.* **2014**, *126*, 13814–13817; b) A. Misra, K. Kozma, C. Streb, M. Nyman, *Angew. Chem. Int. Ed.* **2019**, *0*.
- [4] L. Vilà-Nadal, L. Cronin, *Nat. Rev. Mater.* **2017**, *2*, 17054.
- [5] a) F. M. Toma, A. Sartorel, M. Iurlo, M. Carraro, P. Parisse, C. Maccato, S. Rapino, B. R. Gonzalez, H. Amenitsch, T. Da Ros, L. Casalis, A. Goldoni, M. Marcaccio, G. Scorrano, G. Scoles, F. Paolucci, M. Prato, M. Bonchio, *Nat. Chem.* **2010**, *2*, 826; b) Y. Nishimoto, D. Yokogawa, H. Yoshikawa, K. Awaga, S. Irie, *J. Am. Chem. Soc.* **2014**, *136*, 9042–9052; c) W. Luo, J. Hu, H. Diao, B. Schwarz, C. Streb, Y.-F. Song, *Angew. Chem. Int. Ed.* **2017**, *56*, 4941–4944; *Angew. Chem.* **2017**, *129*, 5023–5026.
- [6] a) J. Lehmann, A. Gaita-Ariño, E. Coronado, D. Loss, *Nat. Nanotechnol.* **2007**, *2*, 312; b) M. Shiddiq, D. Komijani, Y. Duan, A. Gaita-Ariño, E. Coronado, S. Hill, *Nature* **2016**, *531*, 348.
- [7] a) J. Wang, Y. Liu, K. Xu, Y. Qi, J. Zhong, K. Zhang, J. Li, E. Wang, Z. Wu, Z. Kang, *ACS Appl. Mater. Interfaces* **2014**, *6*, 9785–9789; b) A. Misra, I. Franco Castillo, D. P. Müller, C. González, S. Eyssautier-Chuine, A. Ziegler, J. M. de la Fuente, S. G. Mitchell, C. Streb, *Angew. Chem. Int. Ed.* **2018**, *57*, 14926–14931.
- [8] a) C. Streb, R. Tsunashima, D. A. MacLaren, T. McGlone, T. Akutagawa, T. Nakamura, A. Scandurra, B. Pignataro, N. Gadegaard, L. Cronin, *Angew. Chem. Int. Ed.* **2009**, *48*, 6490–6493; *Angew. Chem.* **2009**, *121*, 6612–6615; b) D. Mercier, S. Boujday, C. Annabi, R. Villanneau, C.-M. Pradier, A. Proust, *J. Phys. Chem. C* **2012**, *116*, 13217–13224.
- [9] D.-L. Long, L. Cronin, *Chem. Eur. J.* **2006**, *12*, 3698–3706.
- [10] a) B. Turkot, S. L. Carson, A. Lio, T. Liang, M. Phillips, B. McCool, E. Stenehjem, T. Crimmins, G. Zhang, S. Sivakumar, *Proc. SPIE* **2016**, *9776*, 977602; b) S. Saha, D.-H. Park, D. C. Hutchison, M. R. Olsen, L. N. Zakharov, D. Marsh, S. Goberna-Ferrón, R. T. Frederick, J. T. Diulus, N. Kenane, G. S. Herman, D. W. Johnson, D. A. Keszler, M. Nyman, *Angew. Chem. Int. Ed.* **2017**, *56*, 10140–10144; *Angew. Chem.* **2017**, *129*, 10274–10278; c) S. Goberna-Ferrón, D.-H. Park, J. M. Amador, D. A. Keszler, M. Nyman, *Angew. Chem. Int. Ed.* **2016**, *55*, 6221–6224; *Angew. Chem.* **2016**, *128*, 6329–6332.
- [11] R. D. L. Smith, M. S. Prévot, R. D. Fagan, Z. Zhang, P. A. Sedach, M. K. J. Siu, S. Trudel, C. P. Berlinguette, *Science* **2013**, *340*, 60.
- [12] L. Li, X. Liu, S. Pal, S. Wang, C. K. Ober, E. P. Giannelis, *Chem. Soc. Rev.* **2017**, *46*, 4855–4866.
- [13] J. Stowers, D. A. Keszler, *Microelectron. Eng.* **2009**, *86*, 730–733.
- [14] a) H. Martin, C. K. Ober, *Proc. ACS Div. Polym. Mat.: Sci. Eng.* **1990**, *58*, 908; b) R. T. Frederick, J. T. Diulus, D. C. Hutchison, M. Nyman, G. S. Herman, *ACS Appl. Mater. Interfaces* **2019**, *11*, 4514–4522.
- [15] a) J. Haitjema, Y. Zhang, M. Vockenhuber, D. Kazazis, Y. Ekinici, A. M. Brouwer, *J. Micro. Nanolith.* **2017**, *16*, 033510; b) Y. Zhang, J. Haitjema, M. Baljovic, M. Vockenhuber, D. Kazazis, T. A. Jung, Y. Ekinici, A. M. Brouwer, *J. Photopolym. Sci. Tec.* **2018**, *31*, 249–255.
- [16] N. Mojarad, M. Hojeij, L. Wang, J. Gobrecht, Y. Ekinici, *Nanoscale* **2015**, *7*, 4031–4037.
- [17] J. Stowers, J. Anderson, B. Cardineau, B. Clark, P. D. Schepper, J. Edson, M. Greer, K. Jiang, M. Kocsis, S. Meyers, A. Telecky, A. Grenville, D. D. Simone, W. Gillijns, G. Vandenberghe, *Proc. SPIE* **2016**, *9779*, 977904.
- [18] S. Chakrabarty, C. Ouyang, M. Krysak, M. Trikeriotis, K. Cho, E. P. Giannelis, C. K. Ober, *Proc. SPIE* **2013**, *8679*, 867906.

- [19] A. Cattoni, D. Mailly, O. Dalstein, M. Faustini, G. Seniutinas, B. Rösner, C. David, *Microelectron. Eng.* **2018**, *193*, 18–22.
- [20] a) X. Xing, R. Liu, K. Cao, U. Kaiser, G. Zhang, C. Streb, *ACS Appl. Mater. Interfaces* **2018**, *10*, 44511–44517; b) M. H. Anjass, M. Deisböck, S. Greiner, M. Fichtner, C. Streb, *ChemElectroChem* **2019**, *6*, 398–403.
- [21] Y. Ji, J. Hu, J. Biskupek, U. Kaiser, Y.-F. Song, C. Streb, *Chem. Eur. J.* **2017**, *23*, 16637–16643.
- [22] R. Fallica, J. K. Stowers, A. Grenville, A. Frommhold, A. P. G. Robinson, Y. Ekinci, *J. Micro-Nanolith. Mem.* **2016**, *15*, 033506.
- [23] a) J. Meyer, S. Hamwi, M. Kröger, W. Kowalsky, T. Riedl, A. Kahn, *Adv. Mater.* **2012**, *24*, 5408–5427; b) C. Wu, F. Feng, Y. Xie, *Chem. Soc. Rev.* **2013**, *42*, 5157–5183; c) A. Parasuraman, T. M. Lim, C. Menictas, M. Skyllas-Kazacos, *Electrochim. Acta* **2013**, *101*, 27–40.
- [24] J. Forster, B. Rösner, M. M. Khusniyarov, C. Streb, *Chem. Commun.* **2011**, *47*, 3114–3116.
- [25] F. Marschall, D. McNally, V. A. Guzenko, B. Rösner, M. Dantz, X. Lu, L. Nue, V. Strocov, T. Schmitt, C. David, *Opt. Express* **2017**, *25*, 15624–15634.
- [26] E. Zanchetta, G. D. Giustina, G. Greci, A. Pozzato, M. Tormen, G. Brusatin, *Adv. Mater.* **2013**, *25*, 6261–6265.
- [27] a) A. Cavalleri, T. Dekorsy, H. H. W. Chong, J. C. Kieffer, R. W. Schoenlein, *Phys. Rev. B* **2004**, *70*, 161102; b) F. J. Morin, *Phys. Rev. Lett.* **1959**, *3*, 34–36; c) C. Ko, S. Ramanathan, *J. Appl. Phys.* **2008**, *104*, 086105; d) A. Pergament, G. Stefanovich, V. Andreev, *Appl. Phys. Lett.* **2013**, *102*, 176101.

Manuscript received: July 27, 2020

Accepted manuscript online: August 7, 2020

Version of record online: August 21, 2020